

# The development of a novel coil gun with permanent magnet

Bingxuan Cheng  
American Institute of Aviation  
and Aeronautics(AIAA), Trabuco  
Hill High School,  
Rancho Santa Margarita,CA  
[bingcheng0107@gmail.com](mailto:bingcheng0107@gmail.com)

**Abstract**—In this paper, the development of a novel electromagnetic launcher (coil gun) with permanent magnet (PM) as the projectile is elaborated. The design, calculation, simulation and experimental testing of the PM coil gun are all presented. The coils' energization sequences, the flux distribution, and the corresponding actuation force of the project are all calculated and simulated. The experimental test setup and testing results are also demonstrated. It is concluded that this novel coil gun with permanent magnet can achieve higher speed of projectile, compared to conventional coil gun with ferromagnetic projectile.

**Keywords**— *electromagnetic launcher, coil gun, permanent magnet, simulation, Maxwell, equilibrium point*

## I. INTRODUCTION

An electromagnetic launcher comprises two types: rail gun and coil gun. Due to the inherent disadvantage of contact and wearing problems associated with rail guns and a slow velocity compared to its counterpart, only coil guns are focused upon in this research. The research of coil guns was started and published more than three decades ago (Burgess & Cowan, 1984; Zabar, Naot, Birenbaum, Levi, & Joshi, 1989). Since then, the technology of developing more efficient and powerful coil guns has improved dramatically, primarily due to both a deep understanding of its physics and concepts but also the advancement of electronics and power drivers. The basic principle of a coil gun is to energize and de energize a series of coils around a ferromagnetic projectile (Lee, Kulinsky, Park, Lee, & Kim, 2015; Kondamudi, Thotakura, Pasumarthi, Reddy, Sathyaraj, & Jiang, 2019; Mohamed, Abdalla, Mitkees, & Sabry, 2014; S. Lee, J. Kim, S. Kim 2016; B. Skala, V. Kindl 2014) to accelerate the projectile; with precise timing the projectile can accelerate very quickly, “shooting” out of the electromagnetic launcher at very high speeds. The coil gun's compact setup and high acceleration makes it a suitable candidate for both current and future applications such as gauss guns, kinetic weapon systems, transport of non-life materials, high speed train (Seo, Lim, Choe, Choi, Jeong, 2018) hydraulic piston, and orbital payload launcher (Kaye, Turman, & Shope, 2003).

The main advantage of coil gun with permanent magnet projectile compared to previous design using ferrous iron is that additional flux/energy can be provided from the permanent

magnet and therefore the projectile can be pushed/pulled with higher force which results in higher projectile speed.

This project will research, analyze and test a novel electromagnetic launcher (coil gun) with a permanent magnet (PM) as the projectile. The PM (Neodymium magnet N52), is used instead of a traditional ferromagnetic material to generate more magnetic flux with a higher efficiency, thus increasing its maximum potential. Additionally, a traditional ferromagnetic projectile cannot be “pushed out” by the coil; it only can be “pulled in”; however, with an PM, the coil can exert force of both pulling and pushing, making it substantially more efficient. The concept and potential of this novel EM launcher with a PM will be explored in this study and also compared to the traditional EM launcher with iron, both in simulation, calculation and experimental results.

## II. METHODS

In this section, the theory of the novel EM launcher with a PM is explained; its implementation method and design are described; and both the calculation and simulation results of EM launcher with PM and with iron are also presented, compared and discussed.

### A. Theory

The magnetic flux density  $B_i$  generated from inside of a cylindrical coil is as follows [6]:

$$B_i = \frac{\mu NI}{L} \quad (1)$$

where  $N$  is number of coils turns,  $I$  is the coil current,  $L$  is the axial length of the cylindrical coil, and  $\mu$  is the permeability of the core inside the coil, and in this case, it is  $\mu_0$ , air permeability.

The magnetic flux density  $B_m$  from the axially magnetized permanent magnet is expressed below:

$$B_m = \frac{B_r}{2} \left( \frac{D+z}{\sqrt{R^2+(D+z)^2}} - \frac{z}{\sqrt{R^2+z^2}} \right) \quad (2)$$

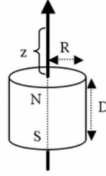


Figure 1 – Dimensions of Axially Magnetized Permanent Magnet

where per the equation and Figure 1 shown above,

$B_r$  : remanence magnetic flux density, intrinsic to the permanent magnet

$Z$ : axial distance from a pole face on the symmetrical axis

$D$ : the height of the cylindrical magnet

$R$ : the radius of the cylindrical magnet

The force exerted on the permanent magnet from the coil current is expressed in the formula below:

$$F = \frac{B_i B_m A}{2\mu_0} \quad (3)$$

where  $B_m$  is the magnetic flux density of the permanent magnet, and  $A$  is the cross-section area of the PM.

Therefore, from the equations above, it can be seen that the electromagnetic force on the projectile (PM) is proportional to the flux density of the PM, which is decided by the size of the PM, the grade of the PM, and the axial distance from the PM, and the flux density generated by the coil. And the coil flux density is proportional to the number of ampere turns of the coil current, and inversely proportional to the axial length of the coil. That is why we need a strong PM, like NdFeB52, which can provide high flux density, high current, more turns of coils.

### B. Design and Implementation

For illustration purposes, the layout and dimensions of our novel coil gun with permanent magnet is shown in Figure 2. Only one set of coils is illustrated here as the starting point of the design, and also for easier explanation purposes. The initial excitation polarity of the coil and the poles orientation of the permanent magnet is also marked in Figure 2.

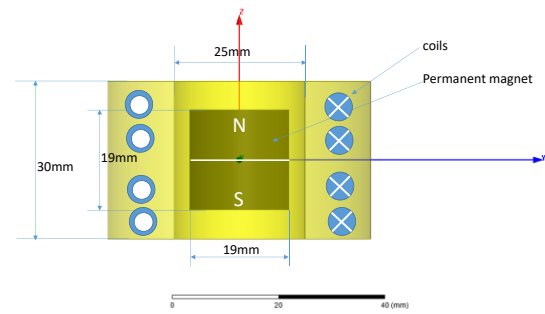


Figure 2 – The layout and dimensions of the coil gun with permanent magnet

The excitation polarities of the coil will be in synchronization with the position of the permanent magnet, and the whole excitation sequence for this single set of coil is listed below:

Step 1: the PM is below the coil, and based on the excitation polarity shown in Figure 3, it is being attracted up by the coil current, and therefore the PM will be moving faster and faster towards the center of the coil due to existing electromagnetic force always being exerted on the projectile.

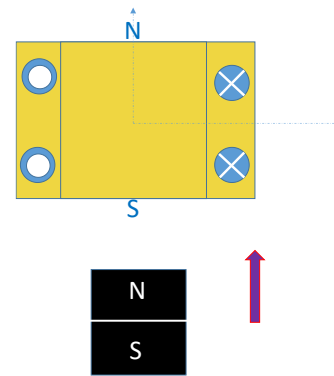


Figure 3 – Step 1 of the actuation sequence of coil gun

Step 2: the PM reaches the center of the coil (the middle line of the PM aligns the middle line of the coil): this is the equilibrium point where the pulling and pushing force from the coil current is equal to each other on the PM, and even there is no absolute force being exerted on the PM at this point, the PM will still be moving up due to the speed momentum generated from step 1.

At this equilibrium point, switch the coil excitation polarity per Figure 4 shown below.

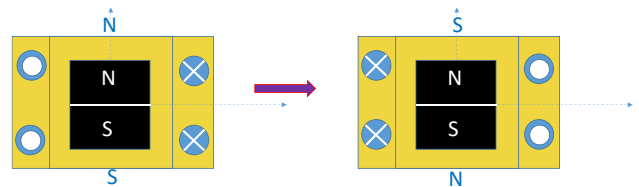


Figure 4 – Step 2 of the actuation sequence of coil gun (from left to right)

Step 3: after step 2, where the excitation polarity of the coil current at the center position is switched, the new magnetic field generated from the coil current will keep pushing the PM out of the coil and therefore the PM will keep moving up faster and faster, as illustrated in Figure 5.

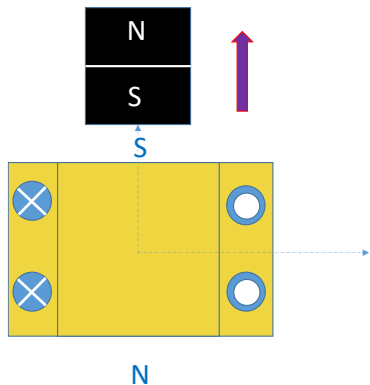


Figure 5 – Step 3 of the actuation sequence of coil gun

### III. SIMULATION AND CALCULATION

Ansys® Maxwell is used as the software for static electromagnetic simulation/computation. Magnetostatic 3D model has been used. Insulating boundary has been applied onto the coils with 4000 Ampere turns of excitation current applied to the coils in the simulation. Neodymium magnet N52 is used in this study, where it has the highest residual flux density of about 1.45 Tesla. The nonlinear residual of the solver is set as 0.001.

#### A. Magnetic Flux Distribution

Figure 6 and Figure 7 below show the magnetic flux distribution from the excited coil and the permanent magnet of the coil gun at the end of step 1, where it can be seen that the strongest flux always resides around the two end surfaces of the PM.

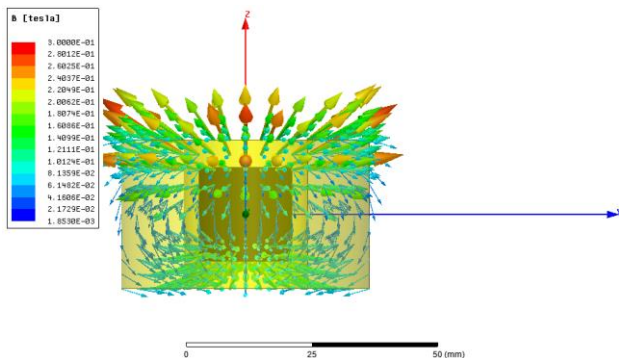


Figure 6 – Magnetic flux distribution from the excited coil

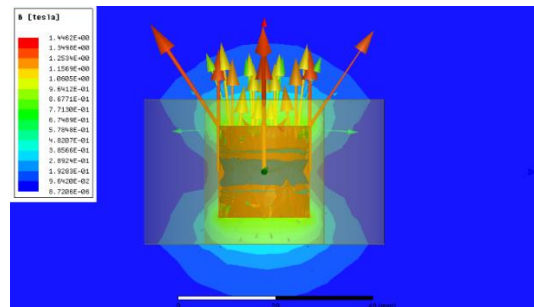


Figure 7 – Magnetic flux distribution from the permanent magnet of the coil gun

#### B. Simulation and Calculation of Single Coil Force and Velocity

Following the 3 steps as introduced in section 2, the force exerted on the PM from the excited coil follows the curve depicted in Figure 8, as calculated from Ansys Maxwell. The distance/gap in the picture is the axial(z) distance between the two center positions of the permanent magnet and the coil. The peak values happens where the PM faces the coils end surface to end surface where the distance in between is the minimum (0) and the PM has the strongest flux density.

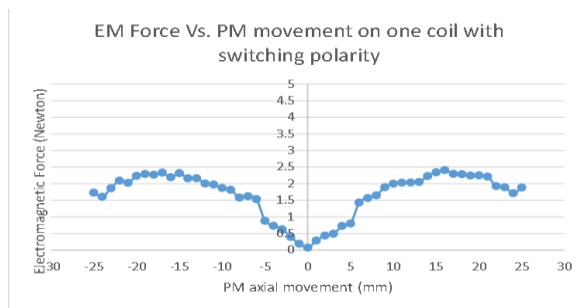


Figure 8 – Electromagnetic Force on PM vs. traveling distance

Figure 8 above clearly shows and proves that the electromagnetic (EM) force on the projectile (PM) from the coil current is always pushing the PM upwards (always positive sign). At the center point(0), the EM force is zero, as explained in section 2, since it is the equilibrium point of the coil and the PM, and after switching the excitation current polarity, the EM force is getting positively higher and higher along the positive upward direction. If the excitation current polarity doesn't change/flip at the center equilibrium point, then the EM force will be negative stronger and stronger and therefore quickly halting the projectile (PM) to a stop.

The energy delivered to the permanent magnet over the 50 mm traveling course from the excited coil is calculated as:

$$E = \int_{-25}^{25} F * dx \quad (4)$$

where  $F$  is the force applied on the permanent magnet, and  $x$  is the distance that PM traveled.

By discretizing the distance over 1mm incremental step, and with the average of the forces over the 1mm step, we can easily calculate the work  $E$  delivered on the permanent magnet over the course of from -25mm to 25mm, which is actually the area under the curve in the Figure 8, and it is calculated as 0.086 Joules accordingly.

For the simplification of calculation, no friction loss (air or contact) during the traveling is included. With this assumption, a formula can be used to calculate the speed of the projectile, as shown in the equation below:

$$E = \frac{1}{2}mv^2 \quad (5)$$

In the equation (5),  $m$  is the mass of the N52 Neodymium magnet, and  $v$  is the final velocity (m/s) of the PM at the end of the course. The mass density of the N52 Neodymium magnet is  $7.45 \text{ g/cm}^3$ , and therefore the mass of the PM is  $m = \text{volume} * \text{density} = 40.1 \text{ grams}$ . Based on the two equations (4 & 5), the final velocity of the projectile (PM) is calculated to be 2 m/s. Therefore, with a single coil stage and only 50 mm of horizontal launching distance, the projectile can reach speeds up to 2 m/s without consideration of friction.

For comparison purposes, the conventional coil gun with the ferromagnetic projectile (such as iron) is simulated here with the same geometry and setup. Without switching coil current polarity, the ferromagnetic projectile travels from -25mm to 25mm along the axial  $z$  axis, and the corresponding electromagnetic force that it receives is shown in the picture below (Figure 9), from which it can be seen clearly that the force profile is very similar to that of PM, but the amplitude of the maximum force is only 0.05 newton, which is 50 times less compared to PM maximum force (2.5 newton). Note: the ferromagnetic projectile can only be pulled by one coil, whilst the PM can be both pulled and pushed, which is drastically more efficient than with the ferromagnetic projectile; the higher energy density of the PM also makes it superior to a ferromagnetic projectile.

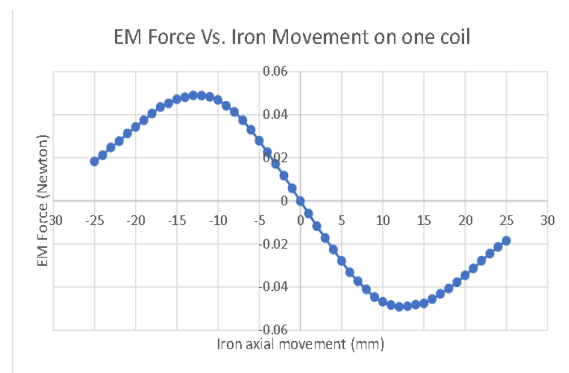


Figure 9 – Electromagnetic Force on Ferromagnet (iron) vs. traveling distance

Based on the same two equations (4 & 5) and the same approach as introduced above the final velocity of the projectile (iron) with a single coil actuation is calculated to be 0.2 m/s, which is only one tenth of the speed of the PM projectile. The negative force exerted is due to the ferromagnet's polarity switching in tandem when the coil switches, as with a PM, that does not occur. If we consider friction in our simulation, the iron speed would be decreased to almost zero.

### C. Dual Coils Simulation and Calculation.

In real applications, multiple coils (2+) have always been used in order to increase the projectile speed further more. In this study, as the simplification purpose, only two sets of coils have been studied here.

Therefore if a second coil is connected on top of the first coil, it can be excited either independently or in synchronization with the first coil to significantly increase the force on the projectile, and therefore significantly increase the velocity of the projectile.

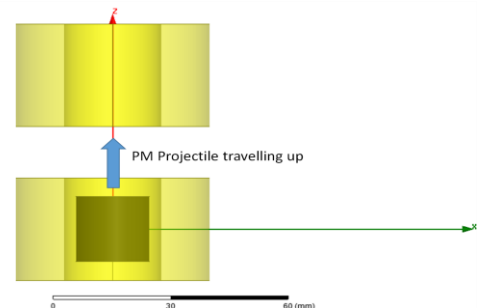


Figure 10 – Simulation Setup of two sets of coils with PM projectile

The case of two sets of identical coils is simulated accordingly in Figure 11, based on Figure 10. The projectile travels from the center of the first coil all the way up towards the center of the second coil. Both coils are excited with the same ampere turns, but with opposite polarities, as shown in Figure 11. Figure 12 shows the EM force profile on the projectile, which demonstrates that the maximum force amplitude is almost doubled compared to the single coil design introduced in Figure 6 & 7.

#### IV. EXPERIMENT AND RESULTS

In this section, the experimental setup and specifications are described in detail, including its mechanical fixture, coil driver, optical sensor, and microcontroller. The experimental speeds of an iron and PM projectile in one and two coils setup are also presented and compared.

##### A. Experiment Setup

The testing setup was done in a glass tube with coils wrapped around it. There were two independently controlled copper coil sets. When the PM triggered the reflective optical sensor, the coil would switch polarity. Since iron cannot get the “push” from the coil, once the iron triggered the sensor, the coil would turn off. This process would then be repeated on to the next coil. A breadboard was used for ease of wiring, and two 3D printed mounts suspended the glass tube and the coils.

An Arduino Uno took analog input from the two CNY70 reflective optical sensors, then output the commands onto two L293N coil/motor drivers. Each motor driver controlled only one coil as the current and voltage needed to be distributed evenly. Matching the simulation, there are 200 turns on each coil and 2 amperes running through each. Figure 14, 15, 16, and 17 are depicting visual representations of key components in the setup.

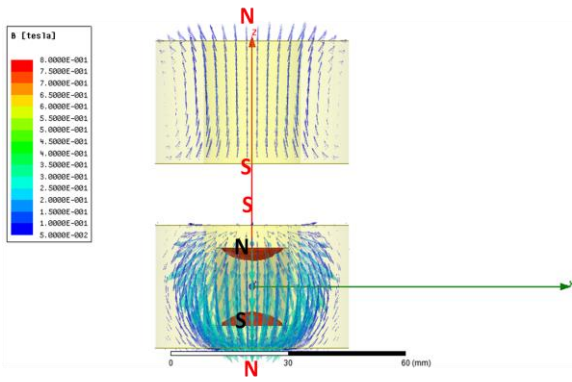


Figure 11 – Magnetic flux distribution from two sets of coils currents at the starting point

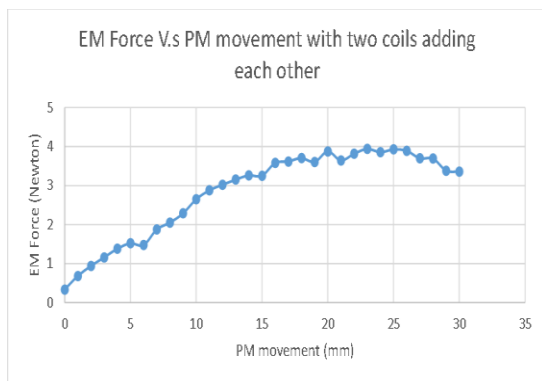


Figure 12 – EM force on the projectile from two sets of coils currents with opposite polarities along the path

If the two sets of coils are excited in the same polarity at the scenario above, then the EM forces from the two coils will cancel each other out, instead of accelerating the PM in the same direction, as shown in Figure 13, where the amplitude of EM force is only about half of the force on the single coil design.

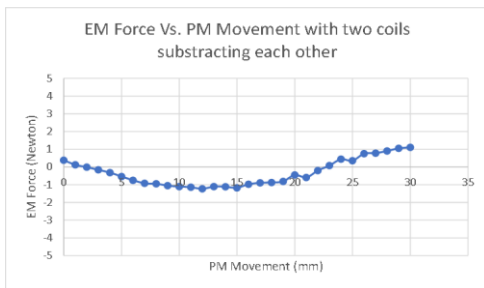


Figure 13 – EM force on the projectile from two sets of coils currents with the same polarity along the path

Based on the same equations and approach as introduced above, the total energy with two coils added along the path is 0.17 Joules, and the speed of the PM projectile after the 2nd coil is calculated to be 2.9 m/s, which is 45% faster than the speed of the one coil’s force PM.

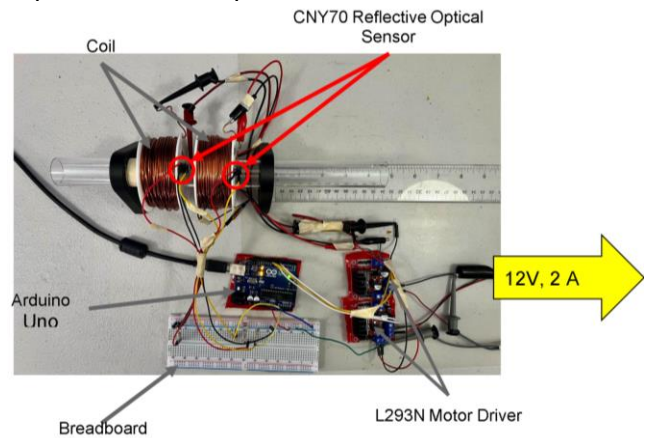


Figure 14 – Diagram of testing setup

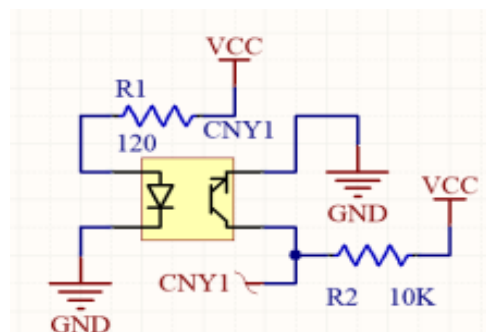


Figure 15 - Schematics of CNY70 reflective optical sensor connection

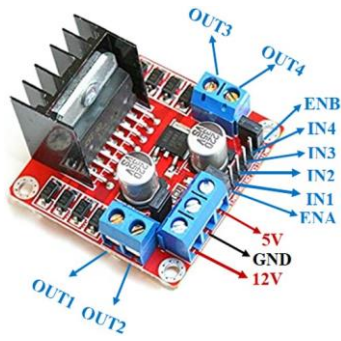


Figure 16 - Pinout Diagram of a L293N motor driver

In order to measure the speed, a “frame distance” measuring technique is used. In simple terms, the projectile is filmed crossing and obstructing a ruler. By calculating the distance the projectile covers in one frame of the recording it is possible to calculate the speed with the frames per second(fps) of the recording. For example, if the object travels 1” in one frame, and the recording is 240 fps, then the object travels 240” per sec, and the value then can be converted at its leisure. The method is accurate enough to confirm our simulations and is cheap to fit the budget of the research. As shown in Figure 14, the ruler is there as reference to calculate the speed.

### B. Experimental Result with Iron

With both coils on, there is insufficient amounts of pulling force, so little that the iron projectile barely travels more than half an inch. This fits the prediction of the simulation, as adding friction on the small force pushing the projectile will definitely slow it to a standstill. With the current environment, the “frame distance method” is not utilized; however, it will be for calculating the speed of the PM.

### C. Experimental Result with Permanent Magnet

A PM was used with a single coil and a dual coil. By using a single coil, the output was ½ inch per frame, and with 240 fps, the final speed of the PM projectile becomes 1.5 m/s. This is close enough to match our simulation, verifying it to be valid. With a dual coil setup, the PM was able to travel up to 1” inch per frame, which is about 3m/s. This does not exactly match the simulation done; however, it completed its sole purpose of validating the simulations.

## V. CONCLUSIONS AND FUTURE WORK

In this paper, the concept of a novel EM launcher with PM has been introduced, and the theory and method of the proposed EM launcher with PM have been explained in detail. Additionally, simulation and experimental results have been completed and discussed. The experimental results, simulation results, and the

theory all coincide with each other, showing that a permanent magnet is drastically more efficient than its ferromagnetic counterpart(10 times in terms of projectile speed) in the application of an EM launcher. The main advantage of using PM as projectile for coil gun over traditional iron coil gun is that PM coil gun can reach higher speed and therefore more power efficient with the same setup as iron coil gun.

Lastly, scaling the electromagnetic launcher also shows a predicted increase of force that matches the simulation's predictions. These findings can help design future electromagnetic launchers with a PM as the payload to store and launch components into orbit.

A youtube link to a video filming one of the multiple PM experiments conducted in this research is listed in the references.(Cheng, 2023)

## REFERENCES

- [1] Burgess T. J., Cowan M. Multistage induction mass accelerator. IEEE Transactions on Magnetics, Vol. 20, Issue 2, 1984, p. 235-238.
- [2] Z. Zabar, Y. Naot, L. Birenbaum, E. Levi, and P.N. Joshi. “Design and Power Condition for the Coil-Gun”, IEEE Transactions on Magnetics, Vol. 25, No.1, Jan 1989.
- [3] S. Lee, L. Kulinsky, B. Park, S. Lee, J. Kim, Design optimization of coil gun to improve muzzle velocity, JOURNAL OF VIBROENGINEERING. MAR 2015, VOLUME 17, ISSUE 2.
- [4] S. Kondamudi, S. Thotakura, M. Pasumarthi, G. Reddy. S. Sathyaraj, X. Jiang, A novel type coil-multipole field hybrid electromagnetic launching system, Results in Physics, 15, 2019.
- [5] H. Mohamed, M. Abdalla, A. Mitkees, W. Sabry, Investigation on Electromagnetic Launching for Single Stage Coilgun, The International Conference on Electrical Engineering 9(9th):1-9, May 2014,
- [6] H. Chai, Electromechanical motion devices, Prentice Hall PTR, ISBN: 0-13-263419-8.
- [7] Cheng, B. (2023, January 21). Testing of a Dual Coil Electromagnetic Accelerator with a Permanent Magnet. YouTube. <https://www.youtube.com/shorts/CeS8rNKyq4w?feature=share>
- [8] R. J. Kaye, B. N. Turman and S. L. Shope, "Applications of coilgun electromagnetic propulsion technology," Conference Record of the Twenty-Fifth International Power Modulator Symposium, 2002 and 2002 High-Voltage Workshop., Hollywood, CA, USA, 2002, pp. 703-707, doi: 10.1109/MODSYM.2002.1189573
- [9] H. Seo, J. Lim, G. -H. Choe, J. -Y. Choi and J. -H. Jeong, "Algorithm of Linear Induction Motor Control for Low Normal Force of Magnetic Levitation Train Propulsion System," IEEE Transactions on Magnetics, vol. 54, no. 11, pp. 1-4, Nov. 2018, Art no. 8207104, doi: 10.1109/TMAG.2018.2842222
- [10] S. Lee, J. Kim, S. Kim, “ Design and experiments of multi-stage coil gun system”, JVE INTERNATIONAL LTD.JOURNAL OF VIBROENGINEERING.JUN 2016, VOL. 18, ISSUE 4. ISSN 1392-8716, pp. 2053-2060
- [11] B. Skala, V. Kindl, “Electromagnetic Coil Gun – Construction and Basic Simulation”, © Springer International Publishing Switzerland 2014, DOI: 10.1007/978-3-319-02294-9-12